

Trace elements supplementation as management tool for anaerobic digestion process

Tina Kegl
 University of Maribor
 Faculty of Chemistry and Chemical
 Engineering
 Maribor, Slovenia
tina.kegl@um.si

Abstract

Waste management and energy crisis are some of the greatest issues that the world is facing today. This problem can be mitigated by anaerobic digestion (AD), where microorganisms in the absence of oxygen produce biogas from organic waste. A useful tool for AD process understanding and optimization is numerical simulation by using mechanistically inspired mathematical models. In this paper, attention is focused on the impact of trace elements in the AD process of a full-scale biogas plant. Special emphasis is put on the optimization of concentrations of trace elements, which are added into the bioreactor in order to improve the produced biogas quantity and quality. Numerical simulation of the AD process is performed by a complex self-developed BioModel, where 187 model parameters are calibrated using an active set optimization procedure. The agreement of the obtained results of numerical simulation in a single CSTR and the measured AD performance over a period of one year, confirms the reliability of the used BioModel and the efficiency of the active set optimization procedure build around a gradient-based algorithm. In order to optimize the amount of added trace elements, three different cases involving various objective and constraints functions are defined. The obtained results show that the optimized amounts of added trace elements enhance the produced biogas essentially by keeping the quality of the biogas within the desired limits. The optimization procedure is numerically efficient, especially if the computation of design derivatives is parallelized.

Keywords: BioModel calibration, active set optimization procedure, approximation gradient-based algorithm

I. INTRODUCTION

Anaerobic digestion (AD) is a promising technology to reduce various types of waste, greenhouse gas emissions to the atmosphere,

and produce renewable energy and other valuable products. During the AD process, microorganisms break down organic matter to biogas and liquid and solid digestate [1,2]. The quantity and quality of produced biogas and digestate depend on adequate process conditions, substrate composition, added additives, heavy metals, and trace elements (TEs) [3-5]. TEs play an important role in chemical, biochemical and physico-chemical processes within the AD process [6]. Recent studies have shown that efficient AD process requires a balanced amount of TEs [7]. Since the substrate of the AD process may lack adequate amount of TEs, TEs supplementation is necessary in order to maintain the AD process efficient. Namely, these bioavailable TEs are necessary micronutrients for the consortium of microorganisms present in AD process [3]. Lack of TEs reduces microbial growth and activity, which can significantly limit the AD process resulting in accumulation of metabolic intermediates, such as volatile fatty acids leading to bioreactor acidification and reduced methane yield. This is especially true for the following TEs: iron (Fe), cobalt (Co), nickel (Ni), selenium (Se), molybdenum (Mo), zinc (Zn), and/or tungsten (W) [7]. Mo, W, and Se are key TEs for action of acetogenic bacteria [8], meanwhile Fe, Zn, and Ni predominance as the methanogens building elements [9]. Some metal TEs, especially Fe, can control the level of H₂S in the produced biogas due to their activities as binding components in forming the sulfide precipitates [10]. Zhang et al. [11] reported that even very high iron concentrations, up to 5.65 gL⁻¹, have no inhibitory effects on the AD process. Xu et al. [12] showed that by proper dosage and particle size of zero-valent iron additives, the CH₄ production and system stability can be improved. Furthermore, by forming sulfide, carbonate, and phosphate precipitates, Fe, Ni, Cu, Ca, Mg, and Co influence also the pH value during AD process and consequently affect the quality and quantity of the produced biogas. On the other hand, excess of essential TEs may also inhibit the AD process [13]. Besides additional process costs, over-supplementation of TEs (i) entails toxicity of TEs with low toxicity threshold concentration, and (ii) restricts down-stream application of digestate as fertilizer due to its TEs contents [14].

These outcomes clearly indicate that predicting the impact of TEs in the AD process is very important in order to obtain required biogas quantity and quality. One way to achieve an adequate balance of TEs is by optimizing the TEs concentration in the substrate. In spite of many investigations of TEs role and fate during the AD process



[7,15,16], there are still gaps in the numerical optimization of the amount of added TEs in the bioreactor.

In this paper, attention is focused on TEs supplementation as a management tool for AD process operation in a full-scale biogas plant. In order to determine the role and impact of these elements on the AD process, the TEs dynamics during AD process is studied by using a self-developed BioModel. The calibrated and validated BioModel is incorporated into the optimization procedure for the improvement of AD performance. Finally, the results of optimized values of added TEs concentrations are presented.

II. EXPERIMENTAL DATA

The operation data used for AD simulation and model calibration were obtained from a full-scale biogas plant Draženci (Slovenia). This plant consists of two equal mesophilic continuously mixed reactors (CSTRs). Both single-stage CSTRs have a hold up of 2500 m³ with one common gas storage facility of 2500 m³. The daily variation of total loading rate of the complex substrate (F-CS) in the CSTRs for a total period of one year is presented in Figure 1.

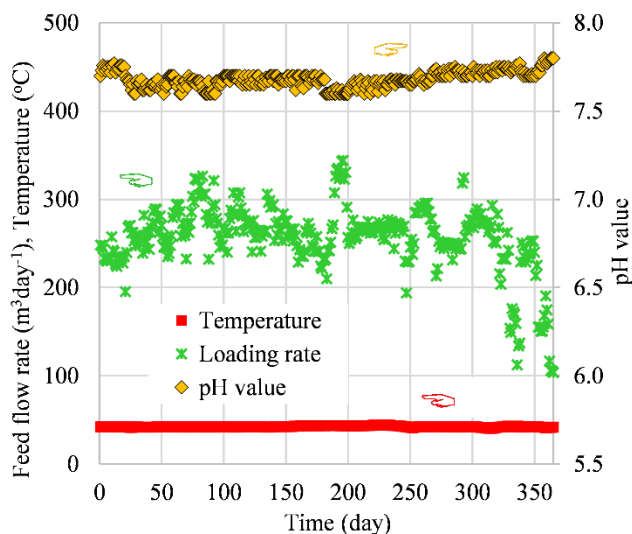


Figure 1. Measured feed flow rate of F-CS, temperature and pH value.

The AD process takes place at a constant pressure of 1.006 bar and average temperature and pH value of 42.5 and 7.68, respectively. The F-CS consists of poultry manure (PM), corn silage (CS), corn meal (CM), fat matter (FM), food waste (FW), and added water (W). The daily variations of fractions of CM, FM, FW, PM, CS, and W are shown for a total period of one year in Figure 2.

The composition of each substrate of F-CS containing TS-total solid, OM-organic matter, ch-carbohydrates, pr-proteins, li-lipids, C_{io}, N_{io}, S_{io}, K_{io}, and P_{io} - inorganic carbon, nitrogen, sulfur, potassium, and phosphorus, and other elements and compounds, Table 1, was determined by the usage of methods prescribed in the corresponding standards.

The concentrations of each TEs in the input substrates F-CS are presented in Figure 3.

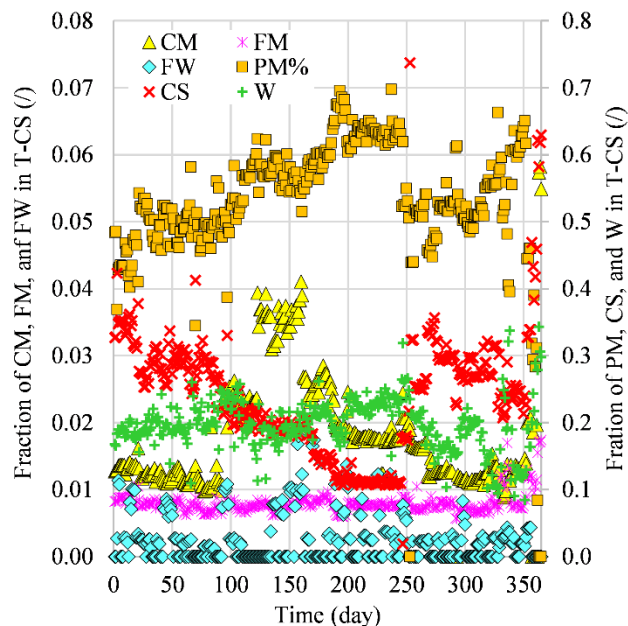


Figure 2. Measured fractions of CM, FM, FW, PM, CS, and W in F-CS.

Table 1. Composition of substrates in F-CS

F-CS	PM	CS	CM	FM	FW
TS (%)	75.73	47.68	65.85	34.12	91.99
OM (% TS)	84.76	96.58	98.35	98.00	98.08
ch (gL ⁻¹)	10.735	6.488	6.438	4.309	31.707
pr (gL ⁻¹)	45.936	33.022	56.970	74.723	66.220
li (gL ⁻¹)	3.555	3.226	19.750	236.312	26.970
C _{io} (gL ⁻¹)	3.57499	2.14185	0.71529	0.13711	42.80220
N _{io} (gL ⁻¹)	1.55322	0.62786	1.08176	1.30420	1.15234
S _{io} (gL ⁻¹)	3.57599	0.06147	0.37446	0.00100	0.98493
K _{io} (gL ⁻¹)	3.23805	1.10575	1.13509	0.04708	2.51013
P _{io} (gL ⁻¹)	2.61164	1.01155	3.54957	0.90058	6.63018
NO ₂ (gL ⁻¹)	0.00871	0.00025	0.00175	0.00003	0.00048
Ca (gL ⁻¹)	3.61388	0.18493	0.02899	1.56674	18.09087
Mg (gL ⁻¹)	0.81457	0.10843	0.30957	0.06587	0.88034
Ni (gL ⁻¹)	0.00052	0.00026	0.00083	0.00110	0.00111
Fe (gL ⁻¹)	0.11026	0.00542	0.01380	0.20543	0.27517
Cr (gL ⁻¹)	0.00346	0.00026	0.00083	0.00250	0.00111
Cu (gL ⁻¹)	0.00991	0.00035	0.00083	0.00238	0.01258
Na (gL ⁻¹)	0.38816	0.00055	0.00746	0.06184	0.50550
Pb (gL ⁻¹)	0.00028	0.00026	0.00083	0.00067	0.00111
Zn (gL ⁻¹)	0.05228	0.00026	0.00535	0.02188	0.13295

To improve the AD process (prevent foaming, and reduce H₂S content in biogas) in the considered biogas plant the following biological and inorganic additives are daily added to the F-CS:

(i) biological additive SensoPower Flex, containing enzymes (cellulase, xylanase, endo-1,4...) to enhance hydrolysis in the AD process, added in the amount of 1500 gday⁻¹

(ii) inorganic additive SensoPower Liquid, containing essential TEs (Co, Cu, Na, Ni, and Se) which are important for a healthy development of microorganisms and enable efficient fermentation as well as prevent foam development, added in the amount of 1.0 Lday⁻¹

(iii) inorganic additive Kemira BDP-840, containing the FeCl_2 to reduce the production of H_2S during the AD process, added in the amount of 100 L day^{-1} .

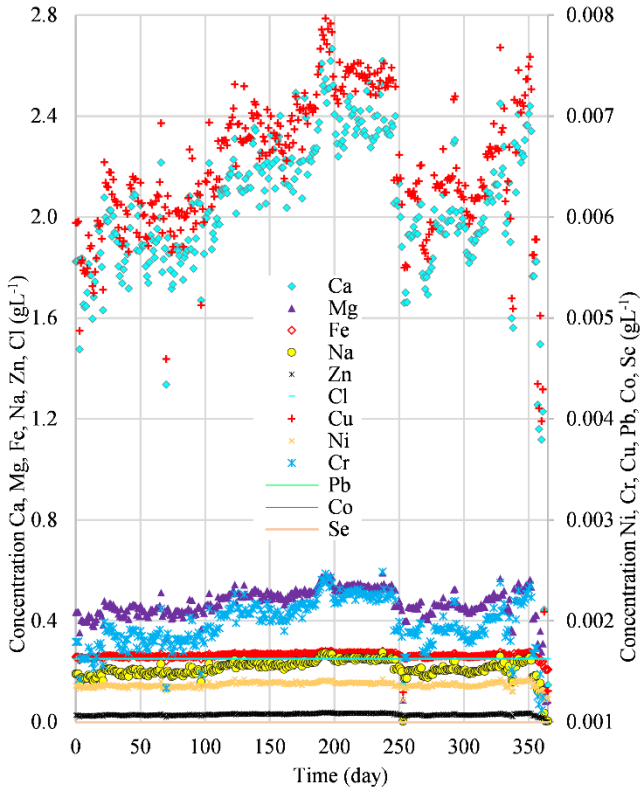


Figure 3. TE in the F-CS.

The total measured unrefined biogas volume is 4375000 m^3 . This biogas contains approximately 54% CH_4 , 45% CO_2 , 60 ppm of H_2 , 200 ppm of H_2S , and 800 ppm of NH_3 , Figure 4.

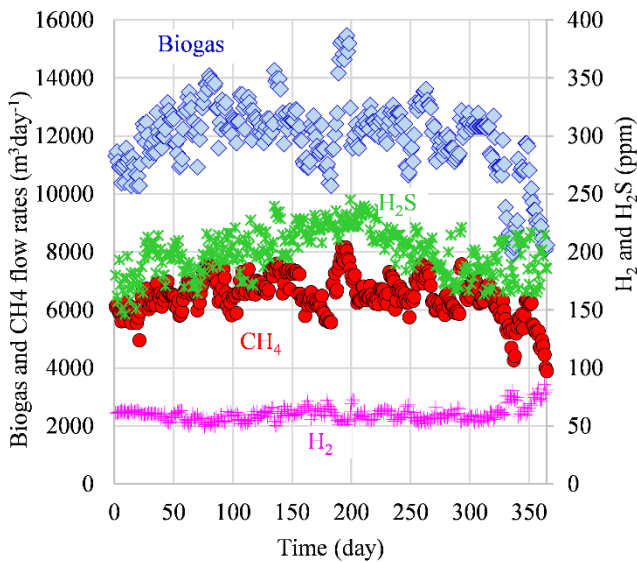


Figure 4. Measured biogas, CH_4 , H_2 and H_2S flow rates in the biogas plant.

The daily variations of the shown data, measured at the plant during the 365 days of the AD process were used to calibrate the model parameters of the BioModel, which was afterwards validated with

the data measured during the subsequent period of 365 days (following the first period) [17,18].

III. OPTIMIZATION OF TRACE ELEMENTS

A. BioModel

In this paper the complex BioModel, which is based on the model presented in [17,18], comprises 80 ordinary differential equations (ODEs) and 54 algebraic equations (AEs). It considers biochemical, chemical, and physicochemical processes. Within biochemical processes, four stages take place: hydrolysis, acidogenesis, acetogenesis, and methanogenesis. Furthermore, the considered physicochemical processes are related to mass transfer from liquid to gas phase and to the precipitation, while chemical processes are related to the acid-base reactions. Finally, the modeling of the activities related to biological and inorganic additives is also incorporated into BioModel. Special attention is focused on the fate of TEs during the AD process. The developed BioModel consist of 187 model parameters, which are unknown or hard-to-determine. In the set of these design variables, the concentrations of enzymes in the F-CS for degrading macromolecules, such are carbohydrates, proteins, and lipids, are also included. These BioModel parameters, which have to be calibrated, can be summarized as follows:

- (i) 3 hydrolysis rate constants, $k_{\text{hyd},i} (\text{day}^{-1})$, $i \in I_{\text{hyd}}$
- (ii) 26 inhibition constants, $K_i (\text{g L}^{-1})$, related to: (a) VFA inhibition of hydrolysis process, $K_{i,\text{VFA}}$, and (b) compounds and metal ions inhibitions of various bacteria growth, $K_{i,\text{H}_2,\text{Agly}}$, $K_{i,\text{H}_2,\text{Aoa}}$, $K_{i,\text{H}_2,\text{Apro}}$, $K_{i,\text{H}_2,\text{S,Apro}}$, $K_{i,\text{H}_2,\text{Abu}}$, $K_{i,\text{H}_2,\text{S,Abu}}$, $K_{i,\text{H}_2,\text{Ava}}$, $K_{i,\text{H}_2,\text{S,Ava}}$, $K_{i,\text{H}_2,\text{S,Mac}}$, $K_{i,\text{NH}_3,\text{Mac}}$, $K_{i,\text{Cu}^{2+},\text{Abu}}$, $K_{i,\text{Zn}^{2+},\text{Abu}}$, $K_{i,\text{Cr}^{2+},\text{Abu}}$, $K_{i,\text{Pb}^{2+},\text{Abu}}$, $K_{i,\text{Ni}^{2+},\text{Abu}}$, $K_{i,\text{Cu}^{2+},\text{Mac}}$, $K_{i,\text{Zn}^{2+},\text{Mac}}$, $K_{i,\text{Cr}^{2+},\text{Mac}}$, $K_{i,\text{Pb}^{2+},\text{Mac}}$, $K_{i,\text{Ni}^{2+},\text{Mac}}$, $K_{i,\text{H}_2,\text{S,Mhyd}}$, $K_{i,\text{H}_2,\text{S,Ss}}$, $K_{i,\text{H}_2,\text{S,Spro}}$, $K_{i,\text{H}_2,\text{S,Sac}}$ and $K_{i,\text{H}_2,\text{S,Shyd}}$
- (iii) 2 limitation factors, $K_M (\text{g L}^{-1})$, of inorganic nitrogen, $K_{M,\text{NiO}}$, and inorganic phosphorus, $K_{M,\text{P}_{10}}$, related to all microbial growth rates
- (iv) 16 Monod saturation constants, $k_M (\text{g L}^{-1})$, related to various substrates and bacteria, $k_{M,\text{suAsu}}$, $k_{M,\text{aaAaa}}$, $k_{M,\text{glyAgly}}$, $k_{M,\text{oaAoa}}$, $k_{M,\text{proApro}}$, $k_{M,\text{buAbu}}$, $k_{M,\text{vaAva}}$, $k_{M,\text{H}_2,\text{Mhyd}}$, $k_{M,\text{acMac}}$, $k_{M,\text{Sio,atSs}}$, $k_{M,\text{proSpro}}$, $k_{M,\text{Sio,atSpro}}$, $k_{M,\text{acSac}}$, $k_{M,\text{Sio,atSac}}$, $k_{M,\text{H}_2,\text{Shyd}}$, $k_{M,\text{Sio,atShyd}}$
- (v) 13 maximal microbial grow rates at optimal temperature, $\mu_{i,\text{max},T_{\text{opt}}} (\text{day}^{-1})$, $i \in I_{\text{bac}}$, 13 microbial decays as a percentage of maximal microbial growth rates $b_{i,\text{dec}}(\%)$, $i \in I_{\text{bac}}$
- (vi) 10 parameters of mass transfer rates from liquid to gas phase, $(K_L a)_{j,a} (\text{°C}^{-1} \text{day}^{-1})$ and $(K_L a)_{j,b} (\text{day}^{-1})$, $j \in I_{\text{gas}}$
- (vii) 17 precipitation rate constants, $k_{\text{cryst}} (\text{day}^{-1})$; $k_{\text{cryst,CaCO}_3}$, $k_{\text{cryst,CuCO}_3}$, $k_{\text{cryst,FeCO}_3}$, $k_{\text{cryst,MgCO}_3}$, $k_{\text{cryst,NiCO}_3}$, $k_{\text{cryst,PbCO}_3}$, $k_{\text{cryst,ZnCO}_3}$, $k_{\text{cryst,CuS}}$, $k_{\text{cryst,FeS}}$, $k_{\text{cryst,NiS}}$, $k_{\text{cryst,PbS}}$, $k_{\text{cryst,ZnS}}$, $k_{\text{cryst,Ca}_3(\text{PO}_4)_2}$, $k_{\text{cryst,Fe}_3(\text{PO}_4)_2}$, $k_{\text{cryst,Ni}_3(\text{PO}_4)_2}$, $k_{\text{cryst,MgNH}_4\text{PO}_4}$, $k_{\text{cryst,KMgPO}_4}$
- (viii) 3 precipitation rate constants of added Co, $k_{\text{cryst}} (\text{day}^{-1})$; $k_{\text{cryst,CoCO}_3}$, $k_{\text{cryst,CoS}}$ and $k_{\text{cryst,Co}_3(\text{PO}_4)_2}$
- (ix) 3 Michaelis-Menten half-saturation constants, $K_{\text{MEO},i} (\text{g L}^{-1})$, $i \in I_{\text{hyd}}$
- (x) 65 parameters related to the growth rate $\mu_j (\text{day}^{-1})$ of j^{th} microbial group: 26 parameters, $\text{p}K_j^{\text{lo}}(\%)$ and $\text{p}K_j^{\text{up}}(\%)$, included into pH functions $f_{\text{pH},j}$, $j \in I_{\text{bac}}$, describing the pH

effects on the growth rate by the Michaelis pH function, which is normalized to give a value of 1.0 as the center value, while 13 parameters, α_j ($^{\circ}\text{C}^{-1}\text{day}^{-1}$), $j \in I_{\text{bac}}$, 13 optimal temperatures, $T_{j,\text{opt}}$ ($^{\circ}\text{C}$), and 13 maximal temperatures, $T_{j,\text{max}}$ ($^{\circ}\text{C}$), $j \in I_{\text{bac}}$, describe the maximal microbial growth rate $\mu_{j,\text{max}}$ (day^{-1}), $j \in I_{\text{bac}}$

- (xi) initial influent concentrations of 13 types of bacteria in the F-CS, X_j (gL^{-1}), $j \in I_{\text{bac}}$
- (xii) concentrations of 3 types of enzymes in the F-CS for degrading carbohydrates, proteins, and lipids, $c_{E0,i}$ (gL^{-1}), $j \in I_{\text{enz}}$.

B. ASO procedure

In order to calibrate 187 model parameters, the active set optimization (ASO) procedure was used [17,18]. The ASO procedure incorporates the used BioModel, a sensitivity analysis and a gradient-based optimization algorithm. The initial values of all design variables are the recommended values from the available literature. The calibration of all BioModel parameters is performed in several cycles. At the beginning of the first cycle, some initial and a relatively high activation threshold value f_T was chosen to determine a relatively low number of active design parameters. Within each cycle, the active design variables x_i^* , for which it holds that the importance factor, obtained by sensitivity analysis, is greater than threshold, $f_{\text{IM},i} \geq f_T$, are determined, while all other design variables are designated as passive in the current cycle. The values of active design parameters are optimized while keeping the passive ones constant at their recommended values. After that a new cycle with a lower value of threshold f_T is started until all design variables are active and calibrated by the optimization process.

C. Optimization procedure

The problem of optimal design can be formulated as: minimize the objective function, subject to constraints and response equation [17]. The response equation is given by the system of equations defining the BioModel; it contains 154 response variables. The objective function relates to the quality of AD performance, while the constraints reflect the imposed limitations. The design variables can be varied independently in order to search for the best possible operation of the AD system. This problem can be verbally expressed as follows: find such values of design variables, that while satisfying the constraints, the value of objective function is minimized.

1) BioModel parameters optimization

To calibrate BioModel parameters, the optimization problem contains 187 design variables and 12 constraints.

The objective function g_0 is defined by Eq. (1), where the differences between experimental data and numerical simulation are minimized

$$g_0 = \sum_i \psi_{0,i} \int_{t_{\text{stab}}}^{t_{\text{total}}} \left(\frac{q_i(t) - q_{i,\text{exp}}(t)}{\bar{q}_{i,\text{exp}}} \right)^2 dt \quad (1)$$

where $\psi_{0,i}$ are normalized weighting factors used to scale the relative importance of individual deviations between q_i and $q_{i,\text{exp}}$; the symbols $q_i(t)$, $q_{i,\text{exp}}(t)$, and $\bar{q}_{i,\text{exp}}$ denote time-dependent calculated, time-dependent measured, and the average values of the measured AD performance of response variable q_i , $i = 1 \dots 5$, $q_i \in I_{\text{obj}} = \{Q_{\text{biogas}}, Q_{\text{g,CH}_4}, Q_{\text{g,H}_2}, Q_{\text{g,H}_2\text{S}}, \text{pH}\}$; where $q_1 = Q_{\text{biogas}}$, $q_2 = Q_{\text{g,CH}_4}$, $q_3 = Q_{\text{g,H}_2}$, $q_4 = Q_{\text{g,H}_2\text{S}}$, $q_5 = \text{pH}$.

The constraints, which are defined in the standard form $g_i \leq 0$, are related to (i) bacteria concentration, Eq. (2), by limiting the concentration below the maximal value of $x_{\text{bac}}^{\text{max}}$, (ii) lower limits of five response variables, $i = 1 \dots 5$, $q_i \in I_{\text{obj}}$, Eq. (3), and (iii) the last six constraints limit the upper values of q_i , $i = 1 \dots 6$, $q_i \in I_{\text{obj}} \cup \{Q_{\text{g,NH}_3}\}$, where $q_6 = Q_{\text{g,NH}_3}$, Eq. (3).

$$g_1 = \frac{\sum_j x_j - x_{\text{bac}}^{\text{max}}}{x_{\text{bac}}^{\text{max}}}, \quad j \in I_{\text{bac}} \quad (2)$$

$$g_{i+1} = \frac{\int_{t_{\text{stab}}}^{t_{\text{total}}} \left(0.5 + \tan^{-1} \left(\frac{10(k_{q_i}^{\text{LO}} q_{i,\text{exp}} - q_i)}{\bar{q}_{i,\text{exp}}} \right) \right) (k_{q_i}^{\text{LO}} q_{i,\text{exp}} - q_i)}{(t_{\text{total}} - t_{\text{stab}}) \bar{q}_{i,\text{exp}}} \quad (3)$$

$$g_{i+6} = \frac{\int_{t_{\text{stab}}}^{t_{\text{total}}} \left(0.5 + \tan^{-1} \left(\frac{10(q_i - k_{q_i}^{\text{UP}} q_{i,\text{exp}})}{\bar{q}_{i,\text{exp}}} \right) \right) (q_i - k_{q_i}^{\text{UP}} q_{i,\text{exp}})}{(t_{\text{total}} - t_{\text{stab}}) \bar{q}_{i,\text{exp}}} \quad (4)$$

where $k_{q_i}^{\text{LO}}$ and $k_{q_i}^{\text{UP}}$ are factors ($k_{q_i}^{\text{LO}} < 1$ and $k_{q_i}^{\text{UP}} > 1$), which define the width of the allowed interval for the i^{th} response variable $q_{i,\text{exp}}$; namely, every considered response variable $q_{i,\text{exp}}$ has to be within the interval $[k_{q_i}^{\text{LO}} q_{i,\text{exp}}, k_{q_i}^{\text{UP}} q_{i,\text{exp}}]$ for any time $t \in [t_{\text{stab}}, t_{\text{total}}]$ [17,18].

2) AD process optimization - optimization of added TEs concentrations

To optimize the amount of added TEs in bioreactor, the TEs concentrations are chosen as design variables. Thus, there are a total of 12 design variables. Three different optimization tasks were formulated. These tasks have the same objective function, Eq. (5) but various constraint functions; these optimization tasks are labeled as Cases A, B, and C.

In Case A only constraints related to the upper and lower values of design variables are considered. In case B, the constraint related to the maximal permissible content of H_2S in the produced biogas, is added, Eq. (6). Besides all these constraints, the constraints related to the allowed lower content of CH_4 and to the upper allowed content of H_2 and NH_3 in biogas are considered in Case C, Eqs. (7)-(9).

The objective function g_0 is defined in order to maximize the total biogas volume V_{biogas} , produced during the duration of the AD process, t_{total} , after the stabilization time, t_{stab} , Eq.(5).

$$g_0 = -\psi \int_{t_{\text{stab}}}^{t_{\text{total}}} V_{\text{biogas}}(t) dt \quad (5)$$

The imposed constraints are related to the minimal prescribed content of CH_4 , Eq. (6), maximal permissible content of H_2 , Eq. (7), of H_2S , Eq. (8), and of NH_3 , Eq. (9), in the produced biogas.

$$g_1 = \psi_1 \left(\varphi_{\text{CH}_4,\text{min}} - \frac{V_{\text{CH}_4}}{V_{\text{biogas}}} \right) \quad (6)$$

$$g_2 = \psi_2 \left(\frac{V_{\text{H}_2}}{V_{\text{biogas}}} - \varphi_{\text{H}_2,\text{max}} \right) \quad (7)$$

$$g_3 = \psi_3 \left(\frac{V_{\text{H}_2\text{S}}}{V_{\text{biogas}}} - \varphi_{\text{H}_2\text{S},\text{max}} \right) \quad (8)$$

$$g_4 = \psi_4 \left(\frac{V_{\text{NH}_3}}{V_{\text{biogas}}} - \varphi_{\text{NH}_3,\text{max}} \right) \quad (9)$$

where $\varphi_{\text{CH}_4,\text{min}}$ denotes minimal fraction of CH_4 , while $\varphi_{\text{H}_2,\text{max}}$, $\varphi_{\text{H}_2\text{S},\text{max}}$, and $\varphi_{\text{NH}_3,\text{max}}$ represent minimal fractions of H_2 , H_2S , and NH_3 in the produced biogas. The symbols V_{biogas} , V_{CH_4} , V_{H_2} , $V_{\text{H}_2\text{S}}$, V_{NH_3} denote volume of biogas, H_2 , H_2S , and NH_3 , while the symbols ψ_i , $i = 1 \dots 4$ are normalized weighting factors.

IV. RESULTS

The BioModel, the ASO procedure and the whole optimization procedure were coded in-house in the C# language. To solve the system of ODEs, the Runge-Kutta and Euler methods are used. The engaged gradient-based optimization algorithm is based on an approximation method [19,20], which sequentially generates approximate strictly convex and separable nonlinear programming problems and solves them to generate a sequence of converging approximate solutions. The algorithm uses the history of design derivatives of the objective and constraint functions to gradually improve the quality of the approximation. Consequently, the convergence is often relatively fast and stable. Since the analytical derivatives can not be obtained easily and any derived formulas would be valid only for a particular AD model form, the numerical differentiation by using simple forward differences was used in this work to get the needed design derivatives.

All numerical simulations were performed using a desktop computer with Inter i7 3.2 GHz CPU with 8 cores. The CPU time for one simulation of the AD process was approximately 1 second, while 1 minute is needed for one full optimization cycle of BioModel parameters calibration, where design derivatives computation was parallelized. The CPU time for one optimization cycle of the AD process (TEs addition) is up to 4 seconds. The number of optimization cycles, needed to obtain optimum BioModel parameters, ranged usually around 100, while around 80 optimization cycles are needed to obtain optimum concentration of added TEs.

A. BioModel calibration

During the BioModel calibration by the ASO procedure, the values of 187 design parameters were allowed to vary between lower and upper limits [17,18]. The values of BioModel parameters are optimized gradually in 4 stages, where the number of active design variables (included in the currently active set) increases by decreasing the threshold. For each set, the selected threshold for, the corresponding number of active design variables, the number of iterations, and the value of the objective function g_0 are given in Table 2. It is evident, that by decreasing the threshold and consequently by including more active design variables in the optimization process, the value of objective function decreases.

Table 2. Sets of active design variables

Set	Threshold f_T	No. of active design variables	No. of iterations	g_0
1	0.1000	16	14	0.12890
2	0.0010	46	41	0.02375
3	0.0001	87	79	0.02042
Optimal	0.0000	187	119	0.02011

In 4th set all BioModel parameters are calibrated; therefore, this design is labeled as optimal design. The comparison of the simulated and measured results is presented only for the period of 365 days, which follows the stabilization period of 135 days.

The simulated biogas and CH₄ flow rates, obtained with the initial and various optimal values of design parameters (computed with active sets 1 to 4; 4 set is labeled as optimal), are compared to the measured data in Figure 5. These flow rates, corresponding to the initial values of design variables, differ from the measured values up to 25% (average absolute daily difference divided by average daily measurement). By increasing the number of active design variables from set to set, the agreement is improved drastically. It is obvious that the simulated biogas flow rates obtained with optimal (calibrated) values of all 187 design parameters, are the closest to the measured data; the average difference is up to 0.5%. After optimizing BioModel parameters, the differences between measured and calculated total biogas and CH₄ volumes are practically negligible.

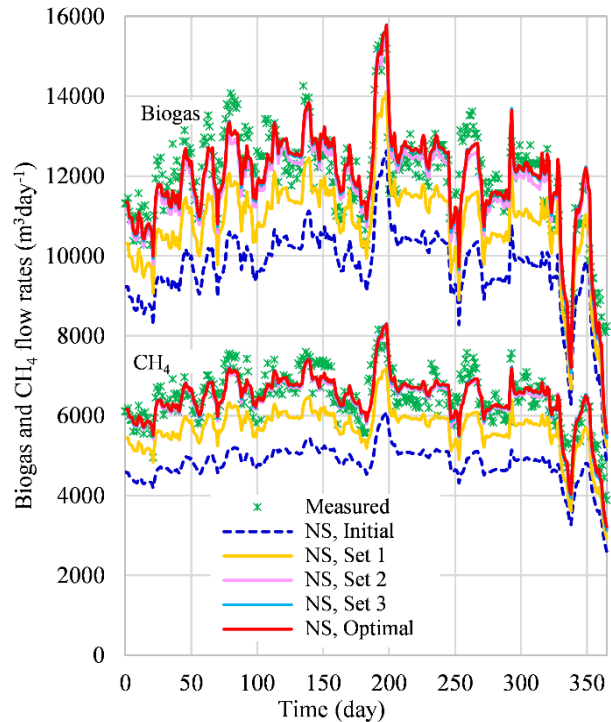


Figure 5. Biogas and CH₄ flow rates (BioModel calibration by ASO procedure)

The simulated H₂ flow rate is compared to the measured data in Figure 6. One can see that the initial difference is substantial, which is improved significantly after optimizing the Sets 1 and 2. Only a minor progress can be observed after optimizing the Set 3 and Set 4. The calculated average H₂ flow rate is up to 20-times higher than the measured one. However, the difference fell to 0.2% after optimizing the Set 4. With fully optimized design parameters, the computed total H₂ volume is practically the same as measured.

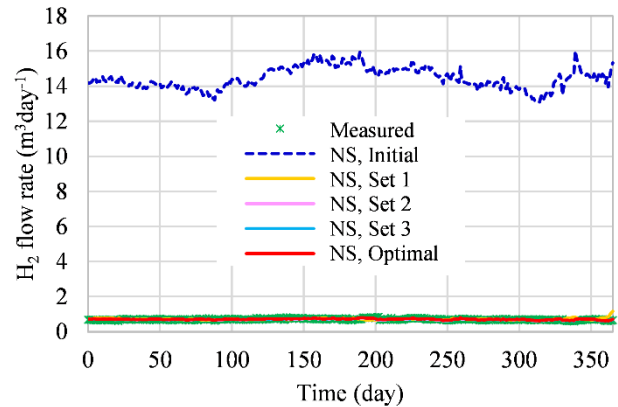
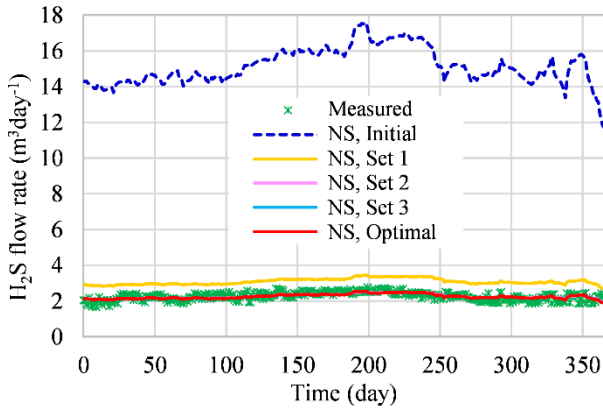


Figure 6. H₂ flow rate (BioModel calibration by ASO procedure)

The simulated H₂S flow rates are compared to measured data in Figure 7. Again, one can see that the initial difference is substantial, which is improved significantly after optimizing the Sets 1 and 2. Again, only a minor progress can be observed after optimizing the Sets 3 and 4. The average difference, being initially around 550%, fell to 0.1% after optimizing the Set 4. With fully optimized design parameters, the computed total H₂S volume differs by about 0.1% from the measured data.


 Figure 7. H_2S flow rate (BioModel calibration by ASO procedure)

The simulated pH values are compared to experimental data in Figure 8. The average difference between simulated and measured values was initially around 5%; after optimizing the Set 4, this difference fell to about 0.06%.

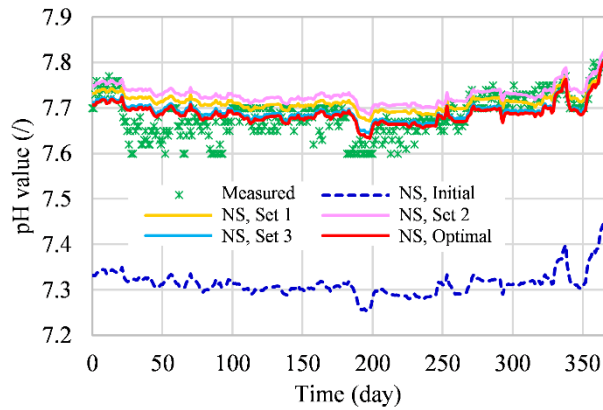


Figure 8. pH value (BioModel calibration by ASO procedure).

During the AD process, pH values influence the concentrations of various species of each TE. As example, the concentration of various Fe species after stabilization time are presented in Figure 9.

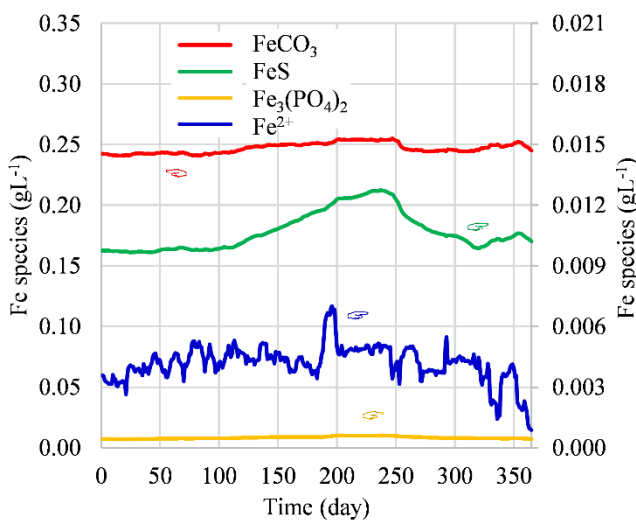


Figure 9. Fe species during AD process at optimal design (BioModel calibration by ASO procedure).

The results of numerical simulations of the AD process by ASO procedure are evaluated by error statistical indicators (SI),

Eqs. (10)-(11), and efficiency statistical indicators, Eqs. (12)-(13). The lower the value of error SI is, the better is the prediction of the model, while the acceptable efficiency SI have to be greater than 0.5.

$$\varepsilon_{MAE} = \frac{1}{n} \sum_{i=1}^n |y_{exp,i} - y_{NS,i}| \quad (10)$$

$$\varepsilon_{RMSE} = \sqrt{\frac{\sum_{i=1}^n (y_{exp,i} - y_{NS,i})^2}{n}} \quad (11)$$

$$R^2 = \left(\frac{\sum_{i=1}^n |y_{exp,i} - \bar{y}_{exp}| |y_{NS,i} - \bar{y}_{NS}|}{\sqrt{\sum_{i=1}^n (y_{exp,i} - \bar{y}_{exp})^2} \sqrt{\sum_{i=1}^n (y_{NS,i} - \bar{y}_{NS})^2}} \right)^2 \quad (12)$$

$$I_{A,rel} = 1 - \frac{\sum_{i=1}^n \left(\frac{y_{exp,i} - y_{NS,i}}{y_{exp}} \right)^2}{\sum_{i=1}^n \left(\frac{|y_{NS,i} - \bar{y}_{exp}| + |y_{exp,i} - \bar{y}_{exp}|}{y_{exp}} \right)^2} \quad (13)$$

where ε_{MAE} ($m^3 day^{-1}$) denotes mean absolute error; ε_{RMSE} ($m^3 day^{-1}$) is root mean square error; $R^2 (/)$ is coefficient of determination, $I_{A,rel} (/)$ is relative index of agreement, n is the number of comparison points, $y_{exp,i}$ and $y_{NS,i}$ are the measured and predicted values of AD performance at i^{th} day of the AD process, respectively; \bar{y}_{exp} and \bar{y}_{NS} are average values of measured and predicted AD performance of the complete AD process, respectively.

Statistical indicators for the most important AD performances from initial design through various sets to the optimal design (calibrated BioModel) are collected in Table 3.

Table 3. Statistical indicators, BioModel calibration

SI	Design	Q_{CH_4}	Q_{H_2}	Q_{H_2S}	Q_{biogas}	pH
ε_{MAE}	Initial	1656.2	13.745	12.896	2237.3	0.3700
	Set 1	790.85	0.0464	0.8309	1149.7	0.0357
	Set 2	262.35	0.0329	0.1401	495.92	0.0474
	Set 3	259.10	0.0306	0.1395	466.43	0.0281
	Optimal	257.61	0.0305	0.1387	467.01	0.0276
ε_{RMSE}	Initial	1695.3	13.739	12.907	2328.7	0.3711
	Set 1	849.93	0.0659	0.8470	1272.6	0.0467
	Set 2	332.74	0.0423	0.1714	632.57	0.0584
	Set 3	329.85	0.0388	0.1706	605.41	0.0368
	Optimal	326.62	0.0387	0.1702	604.38	0.0354
R^2	Initial	0.7958	0.4116	0.6056	0.7995	0.5693
	Set 1	0.8244	0.4496	0.6182	0.8341	0.5883
	Set 2	0.8280	0.5198	0.6202	0.8380	0.5943
	Set 3	0.8286	0.5670	0.6272	0.8398	0.6066
	Optimal	0.8288	0.5959	0.6290	0.8404	0.6169
$I_{A,rel}$	Initial	0.4354	0.0050	0.0300	0.5582	0.1667
	Set 1	0.6913	0.2272	0.3378	0.7844	0.6180
	Set 2	0.9312	0.6355	0.7296	0.9356	0.6527
	Set 3	0.9336	0.7052	0.7392	0.9422	0.6733
	Optimal	0.9338	0.7087	0.7433	0.9483	0.6797

From Table 3, it is evident that error SI decreases from the initial to the final active set gradually, while the efficiency SI gradually increases; all SI values are acceptable.

B. Optimization of trace elements

The initial design of AD process optimization (optimization of added TEs amounts) is the same as it was obtained by BioModel calibration; the AD performance agree very well with experimental data; in the initial design there are no added TEs. For the AD process optimization the concentrations of all included TEs can be

varied within specified intervals. The lower values of all TEs are equal to zero, while the upper limits of Ca, Mg, Ni, Fe, Cr, Cu Na, Cl, Co, and Se are equal to 1.0 gL⁻¹, and of Zn and Pb are equal to 0.1 gL⁻¹. The obtained optimal values of the concentration of added TEs are presented in Figure 10. In Case A, the biogas volume is maximized by higher concentrations of Ca, Mg, Fe, and Co, followed by Ni and Cu. The obtained results in Case B show that the limited content of H₂S in biogas can be reached by the highest content of Fe, followed by lower concentration of added Mg and Co, while Zn should be added in a negligible amount. Furthermore, the maximization of the produced biogas in Case C requires also the addition of Fe. Besides the highest amount of Fe, Mg and Co should be also added in a notable content, while the Ca, Ni, and Cu should be added in rather small amounts.

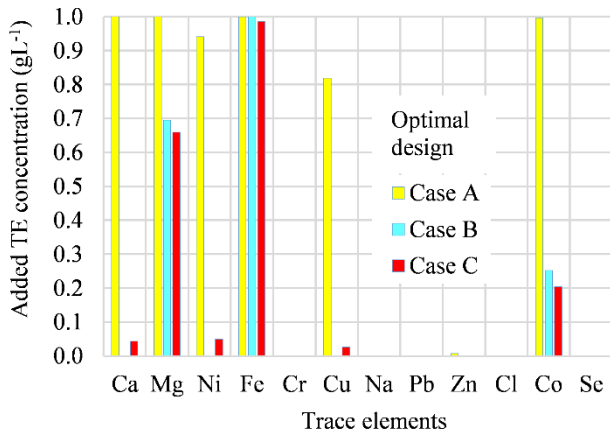


Figure 10. Optimal concentration of added TEs.

The produced biogas and its components in all cases of optimization are shown in Figure 11. The highest produced volumes of biogas and CH₄ are reached in Case A, where no constraints are considered. It has to be pointed out that in this case the volume of H₂S increased also. In Cases B and C the calculated cumulative volumes of biogas and CH₄ are quite similar.

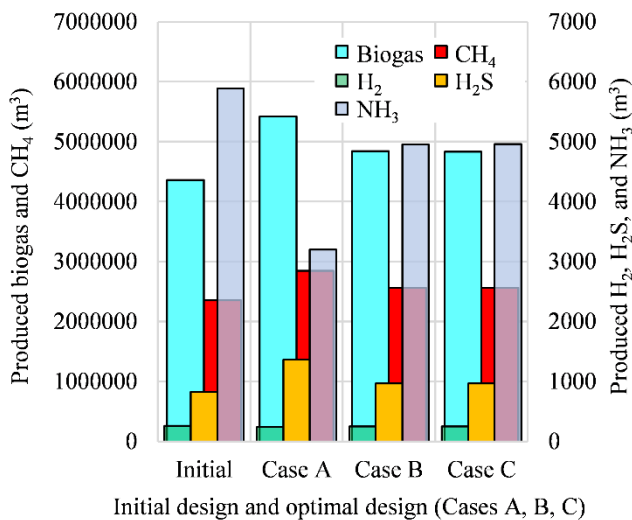


Figure 11. Initial and optimal cumulative production of biogas, CH₄, H₂, H₂S, and NH₃

Finally, Figure 12 shows the variation in cumulative volume of biogas, CH₄, H₂, H₂S, and NH₃ in Cases A, B, and C with respect to the initial design. The obtained results show, that the highest increase of biogas and CH₄ production is reached in Case A. Namely, this production increased by 25%. Unfortunately, the

content of H₂S increases also with respect to the initial design. The optimal AD performance in cases B and C is quite similar. It has to be pointed out, that these similar results are obtained by different optimized concentrations of various added TEs, Figure 10.

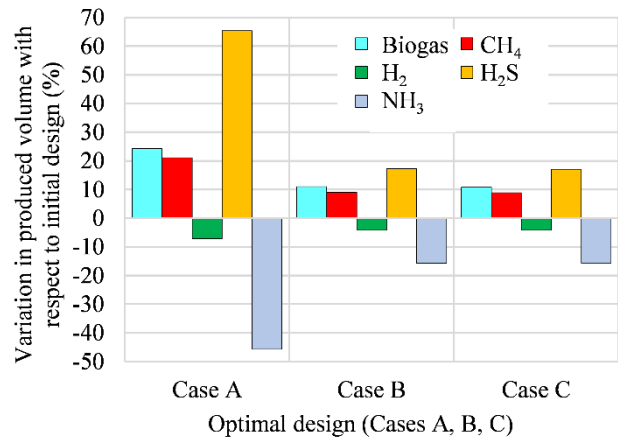


Figure 12. Variation in cumulative volume of biogas, CH₄, H₂, H₂S, and NH₃ with respect to initial design

The obtained results of the AD process optimization (Cases A, B, and C) confirm that Fe determines the efficiency of the AD process most significantly [14]. Fe plays an important role in the formation of various precipitates, especially in forming sulfides, which reduce H₂S content in biogas; the addition of other metals, such as Ni, Co, and Cu, can help to reduce H₂S also. The dynamic of various Fe species concentrations in Case C during total AD duration, including stabilization time, are presented in Figure 13.

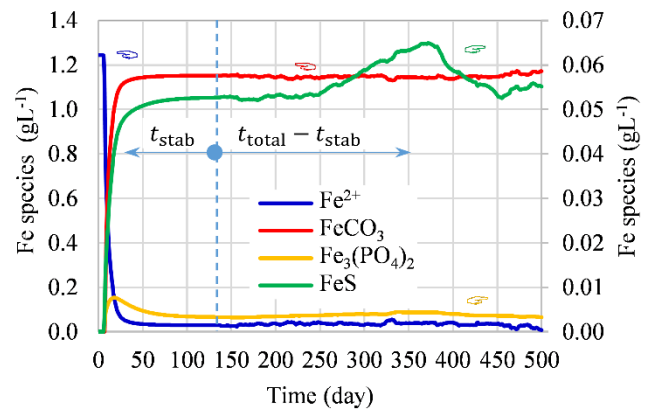


Figure 13. Fe species during AD process at optimal design C.

In Case C, Mg also dictates the production of biogas and other co-products to some extent. Namely, Mg forms precipitates, as carbonate MgCO₃, struvite MgNH₄PO₄, and k-struvite KMgPO₄, which affects pH value, and consequently bacteria growth and biogas quantity and quality. As example, the dynamics of various Mg species concentrations during stabilization period and total time of simulation are shown in Figure 14.

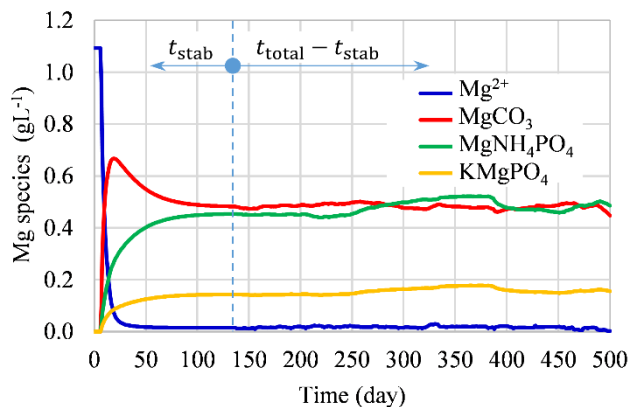


Figure 14. Mg species during AD process at optimal design C.

V. CONCLUSIONS

The complex BioModel, which includes biochemical, chemical, and physicochemical processes in bioreactor during the AD process, is included into the optimization procedure for BioModel calibration using the ASO procedure. After the calibration and validation of the BioModel by experimental data of a full-scale biogas plant, the BioModel is included into the optimization procedure of the AD process. In this context, three optimization problems are defined. The obtained results show that by optimized values of added TEs, especially Fe, Ni, and Co, the biogas quantity as well as quality can be improved.

The proposed optimization of the amounts of added TEs could be extended by optimizing the feedstock composition, feeding strategy, and AD process parameters. Furthermore, the management of biogas to produce electricity, fuels, and chemicals as well as nutrient recovery from the AD digestate could be included in the definition of the optimization problem.

VI. ACKNOWLEDGMENTS

The author is grateful for the financial support of the Slovenian Research Agency (core research funding No. P2-0414). The author also highly appreciates the fellowship granted by L'Oréal-UNESCO, Slovenia, under the program "For Women in Science 2022".

VII. REFERENCES

- [1] I. Angelidaki, L. Ellegaard, B.K. Ahring, "A comprehensive model of anaerobic bioconversion of complex substrates to biogas," *Biotechnology and Bioengineering*, vol. 63(3), pp. 363-372, 1999.
- [2] D.J. Batstone, J. Keller, I. Angelidaki, S.V. Kalyuzhnyi, S.G. Pavlostathis, A. Rozzi, W.T.M. Sanders, H. Siegrist, V.A. Vavilin, *Anaerobic Digestion Model No. 1 (ADM1)*. London: IWA Publishing, 2002.
- [3] B.C. Maharaj, M.R. Mattei, L. Frunzo, E.D. van Hullebusch, G. Esposito, "A general framework to model the fate of trace elements in anaerobic digestion environments," *Scientific Reports* vol. 11, no. 7476, 2021. <https://doi.org/10.1038/s41598-021-85403-2>.
- [4] T. Kegl, A. Kovač Kralj, "Multi-objective optimization of anaerobic digestion process using a gradient-based algorithm," *Energy Conversion and Management*, vol. 226, no. 113560, 2020. <https://doi.org/10.1016/j.enconman.2020.113560>.
- [5] T. Kegl, "Consideration of biological and inorganic additives in upgraded anaerobic digestion BioModel," *Bioresour. Technology*, vol. 355, no. 127252, 2022a. <https://doi.org/10.1016/j.biortech.2022.127252>.
- [6] S. Myszograj, A. Stadnik, E. Pluciennik-Koropczuk, "The Influence of Trace Elements on Anaerobic Digestion Process", *Civil and Environmental Engineering Reports*, vol. 28, no. 4, pp. 105-115, 2018. <https://doi.org/10.2478/ceer-2018-0054>.
- [7] L. Frunzo, F.G. Feroso, V. Luongo, M.R. Mattei, G. Esposito, "ADM1-based mechanistic model for the role of trace elements in anaerobic digestion processes," *Journal of Environmental Management*, vol. 241, pp. 587-602, 2019. <https://doi.org/10.1016/j.jenvman.2018.11.058>.
- [8] B. Wintsche, K. Glaser, H. Sträuber, F. Centler, J. Liebetrau, H. Harms, S. Kleinsteuber, "Trace elements induce predominance among methanogenic activity in anaerobic digestion," *Frontiers in Microbiology*, vol. 7, 2034, 2016. <https://doi.org/10.3389/fmicb.2016.02034>.
- [9] Y. Y. Choong, I. Norli, A. Z. Abdullah, M. F. Yhaya, "Impacts of trace element supplementation on the performance of anaerobic digestion process: A critical review," *Bioresour. Technology*, vol. 209, pp. 369-379, 2016. <https://doi.org/10.1016/j.biortech.2016.03.028>.
- [10] P.M. Thanh, B. Ketheesen, Z. Yan, D. Stuckey, "Trace elements speciation and bioavailability in anaerobic digestion: A review," *Biotechnology Advances*, vol. 34, pp. 122-136, 2016. <https://doi.org/10.1016/j.biotechadv.2015.12.006>.
- [11] H. Zhang, Y. Tian, L. Wang, X. Mi, Y. Chai, "Effect of ferrous chloride on biogas production and enzymatic activities during anaerobic fermentation of cow dung and *Phragmites* straw. *Biodegradation*," vol. 27, pp. 69-82, 2016. <https://doi.org/10.1007/s10532-016-9756-7>.
- [12] W. Xu, F. Long, H. Zhao, Y. Zhang, D. Liang, L. Wang, K. Larson Lesnik, H. Cao, Y. Zhang, H. Liu, "Performance prediction of ZVI-based anaerobic digestion reactor using machine learning algorithms," *Waste Management*, vol. 121, pp. 59-66, 2021. <https://doi.org/10.1016/j.wasman.2020.12.003>.
- [13] E. D. van Hullebusch, G. Guibaud, S. Simon, M. Lenz, S. S. Yekta, F. G. Feroso, R. Jain, L. Duester, J. Roussel, E. Guillon, U. Skjellberg, C. M. R. Almeida, Y. Pechaud, M. Garuti, L. Frunzo, G. Esposito, C. Carliell-Marquet, M. O. G. Collins, "Methodological approaches for fractionation and speciation to estimate trace element bioavailability in engineered anaerobic digestion ecosystems: An overview," *Critical Reviews in Environmental Science and Technology*, vol. 46, pp. 1324-1366, 2016. <https://doi.org/10.1080/10643389.2016.1235943>.
- [14] B.C. Maharaj, M.R. Mattei, L. Frunzo, E.D. van Hullebusch, G. Esposito, "ADM1 base mathematical model of trace element precipitation/dissolution in anaerobic digestion processes," *Bioresour. Technology*, vol. 267, pp. 666-676, 2018. <https://doi.org/10.1016/j.biortech.2018.06.099>.
- [15] B.C. Maharaj, M.R. Mattei, L. Frunzo, E.D. van Hullebusch, G. Esposito, "ADM1 based mathematical model of trace element complexation in anaerobic digestion processes," *Bioresour. Technology*, vol. 276, pp. 253-259, 2019. <https://doi.org/10.1016/j.biortech.2018.12.064>.
- [16] T. Kegl, A. Kovač Kralj, "An enhanced anaerobic digestion BioModel calibrated by parameters optimization based on measured biogas plant data," *Fuel*, vol. 312, no. 122984, 2022. <https://doi.org/10.1016/j.fuel.2021.122984>.
- [17] T. Kegl, "Calibration of anaerobic digestion BioModel by using multi-objective optimization and full-scale biogas plant data," *IEECP Conference 2022, Oxford, 2022b*, <https://sci-index.com/DAI/2022.99101/IEECP/20220189>.
- [18] M. Kegl, M.M. Oblak, "Optimization of mechanical systems: on non-linear first-order approximation with an additive convex term," *Communications in Numerical Methods in Engineering*, vol. 13, pp. 13-20, 1997. [https://doi.org/10.1002/\(SICI\)1099-0887\(199701\)13:1<13::AID-CNM33>3.0.CO;2-E](https://doi.org/10.1002/(SICI)1099-0887(199701)13:1<13::AID-CNM33>3.0.CO;2-E).
- [19] M. Kegl, B.J. Butinar, B. Kegl, "An efficient gradient-based optimization algorithm for mechanical systems," *Communications in Numerical Methods in Engineering*, vol. 18, pp. 363-371, 2002. <https://doi.org/10.1002/cnm.499>.
- [20] F.G. Feroso, E. van Hullebusch, G. Collins, J. Rousef, A.P. Mucha, G. Esposito, "Trace elements in Anaerobic Biotechnologies," IWA Publishing, London, 2019. <https://doi.org/10.2166/9781789060225>.